RSC Advances

PAPER

View Article Online
View Journal | View Issue

Cite this: *RSC Adv.*, 2014, **4**, 50123

Promoting effect of dual modification of H-ZSM-5 catalyst by alkali treating and Mg doping on catalytic performances for alkylation of benzene with ethanol to ethylbenzene

Wen Ding,[a] Yuyang Cui,[a] Jianjun Li,[a] Yiquan Yang[b] and Weiping Fang*[a]

Received 31st July 2014
Accepted 29th September 2014

DOI: 10.1039/c4ra07918c

www.rsc.org/advances

Alkali-treated HZSM-5 zeolite (AT) was modified with Mg species to produce combined modified HZSM-5 catalyst (Mg-AT) for alkylation of benzene with ethanol to ethylbenzene. The catalysts were tested and characterized by X-ray diffraction (XRD), NH_3-Temperature Programmed Desorption (NH_3-TPD), Nitrogen adsorption–desorption, Magic angle spinning nuclear magnetic resonance (MAS NMR) and Scanning Electron Microscope (SEM) techniques. The characterization results showed that for the combined modified HZSM-5 sample, the ratio of surface area of mesopores to the total surface area was the highest. The Mg (1 wt%)-AT catalyst was found to exhibit the highest activity (30% of the conversion of benzene) and selectivity to EB (92%) for the reaction, which was confirmed to be due to the proper *L*/*B* acid proportion (3.79) and the improvement of the mesopores of the catalyst.

1. Introduction

Ethylbenzene (EB) is a very important chemical raw material, mainly used for the production of styrene. Alkylation of benzene with ethylene is a vital reaction for producing ethylbenzene.[1] HZSM-5 zeolite catalysts were believed to be optimal catalysts for ethylbenzene production because of their high surface area, high thermal stability and eco-friendly nature[2–7] compared to conventional homogeneous catalysts such as aluminum chloride or phosphoric acid. Lately, the direct use of ethanol, instead of ethylene, as a benzene alkylating agent gained more attention because ethanol could prolong zeolite catalyst life. Also, the countries and regions with lower ethylene production capacity can derive industrial ethanol from biomass as a raw material for the manufacture of chemicals.[2,8–11]

In the reaction of converting benzene to ethylbenzene, zeolite (HZSM-5) has been used as a catalyst. It is well-known that the alkylation reaction of benzene in the presence of an acid catalyst belongs to a carbenium ion type mechanism, and both Brønsted acid site and Lewis acid site are the active sites.[12,13]

In general, unmodified HZSM-5 catalysts have numerous micro-porous void spaces and strong acidic sites, leading to the generation of secondary products like dimethylbenzene. These two drawbacks result in lower selectivity and a variety of secondary reactions in the alkylation process.[14–18] Currently, alkali-treatment of ZSM-5 was found to change the void fraction of the HZSM-5 sample, leading to an increase in the number of adsorption sites.[19–23] Another way to improve selectivity toward ethylbenzene is to change the acidity of ZSM-5 by introducing an additive compound into the zeolite system.[24–26] For example, HZSM-5 zeolite was modified with H_3BO_3 or H_3PO_4 to eliminate strong acid sites on the surface to achieve higher ethylbenzene selectivity.[7] Also, zinc-containing ZSM-5 could be prepared by incipient wetness impregnation, ion exchange in aqueous solution and chemical vapor deposition techniques.[27] MgO was also introduced into HZSM-5 to reduce strong acid sites and increase Lewis acid sites.[28,29] However, developing a ZSM-5 catalyst with alkali-treatment combined with the addition of Mg promoter for the modification of benzene alkylation with ethanol has not been investigated in detail.

In this study, HZSM-5 zeolite was modified by both alkali treatment and introducing different amounts of Mg species. Both the stability and the catalytic activity of the combined modified HZSM-5 catalysts for the alkylation of benzene with ethanol to ethylbenzene were examined. Moreover, the acid property of the modified ZSM-5 catalysts was investigated by NH_3-TPD and pyridine IR techniques. Nitrogen adsorption–desorption, magic angle spinning nuclear magnetic resonance (MAS NMR) and SEM techniques were also employed to study the change of pore structure.

[a]*Department of Chemical and Biochemical Engineering, College of Chemistry and Chemical Engineering, Xiamen University, Xiamen, 361005, PR China. E-mail: wpfang@xmu.edu.cn; Fax: +86-592-2186291; Tel: +86-592-2186291*

[b]*Department of Chemistry, College of Chemistry and Chemical Engineering, National Engineering Laboratory for Green Chemical Productions of Alcohols, Ethers and Esters, Xiamen University, Xiamen, 361005, PR China*

2. Experimental methods

2.1 Catalyst preparation

HZSM-5 catalyst was prepared as follows: the purchased NH_4-ZSM-5 (the mole ratio of SiO_2 to Al_2O_3 is 80) powder (supplied by Nan Kai Chemical Plant) was directly calcined at 823 K for 2 h to obtain HZSM-5.

The alkali-treated HZSM-5 zeolite (hereafter abbreviated to HZSM-5-AT) was prepared by a conventional method described in literatures elsewhere.[30–33] In brief, appropriate amount of NH_4-ZSM-5 was suspended in 0.2 mol L^{-1} NaOH solution at 338 K for 2 h under stirring and refluxing to produce a mixture, which was then cooled and filtered, followed by washing with deionized water three times to eliminate Na^+. Finally, the as-prepared zeolite samples were dried at 383 K in an air oven overnight and calcined at 823 K for 4 h. One gram of the sample prepared above was mixed with 20 mL of 0.5 mol L^{-1} NH_4NO_3 solution, keeping the mixture at 358 K in a water bath for 2 h under stirring, followed by washing the mixture with deionized water three times to create a cation-replaced ZSM-5 sample, NH_4-ZSM-5-AT; finally, the NH_4-ZSM-5-AT sample was dried at 383 K, then calcined at 823 K for 2 h to produce HZSM-5-AT.

The magnesium-modified HZSM-5 zeolites Mg-HZSM-5-AT (hereafter abbreviated to Mg-AT) and Mg-HZSM-5 (hereafter abbreviated to Mg–H) were prepared by an isovolumetric impregnation method. An appropriate amount of HZSM-5-AT or HZSM-5 was immersed into $Mg(NO_3)_2$ solution under stirring for 2 h at ambient temperature, followed by evaporating, drying, and finally calcining at 823 K in air for 4 h to obtain the target catalysts, the ratio of the amount of loaded Mg to that of the zeolite was 0.3 wt%, 1 wt%, 5 wt% or 7.5 wt%. The catalysts obtained were designated as Mg (0.3 wt%, 1 wt%, 5 wt% or 7.5 wt%)-AT and Mg (0.3 wt%, 1 wt%, 5 wt% or 7.5 wt%)-H, depending on the respective zeolites and the amount of promoter used.

All zeolite samples produced above were broken and sieved, and the pellets with 30–60 mesh were collected for further use.

2.2 Catalytic activity testing

The activity of the catalyst was tested in a continuous stainless steel tubular flow fixed-bed micro-reactor, wherein 2 g of the catalyst with 30–60 mesh was packed. Before catalytic activity test, high-purity N_2 (99.999% purity) was introduced into the system and the temperature was raised to 723 K for 2 h. Then the temperature was decreased to 653 K. Subsequently, benzene and ethanol (molar ratio is 4 : 1) with WHSV (weight hourly space velocity) of the mixture at 4 h^{-1} were pumped into the reactor by a SZB-2 double column trace pump at atmosphere pressure to start the reaction. The product was analyzed by a GC-950 gas chromatograph (Shanghai haixin chromatographic instrument co., LTD) equipped with a flame ionization detector (FID) and HP-5 gas phase capillary column (25 m × 0.25 mm).

2.3 Catalyst characterization

X-ray diffraction (XRD) measurements were performed on a PANalytical X′ pert PRO X-ray diffractometer utilizing monochromatic Cu kα radiation and scanning 2θ range from 10° to 80°, with a scanning step length of 0.0167°.

N_2 adsorption–desorption analysis data were obtained at 77 K using a physical adsorption instrument (Micromeritics Tristar 3000). Before measurement, the samples were pretreated at 300 °C for 3 h under vacuum. The total surface area was evaluated using BET method; and *t*-plot method was used in evaluating the microspore surface area and pore volume. Mesopore distribution was obtained according to the BJH method.

^{27}Al MAS NMR spectra were measured at 78.2 MHz with 5000 Hz of spinning frequency and 1 μs of pulse width, and scans were made 100 times at interval of 360 s.

The surface morphology was observed by using a scanning electron microscope (SEM, Hitachi S-3400N). The samples for SEM imaging were coated with a thin layer of gold film to avoid charging.

The acidity of the catalysts was measured by temperature-programmed desorption of ammonia (NH_3-TPD) on a self-constructed instrument equipped with a quadrupole mass spectrometer model QIC-20 (Hiden Analytical Co, Ltd). Before adsorption, the catalyst (100 mg) was pretreated at 773 K in dry air flow for 2 h, then cooled down to 313 K and saturated with a gas mixture of 10% NH_3/Ar for 1 h. After purging away gaseous NH_3 with Ar, the sample was heated to 823 K at a ramping rate of 10 K min^{-1}. Desorption signals were recorded by monitoring $m/z = 16$.

IR spectra of the samples were recorded using a FT-IR spectrometer (WQF-410). The samples were analyzed in the wavelength range of 4000–400 cm^{-1}.

3. Results and discussion

3.1 Physicochemical characterization

N_2 adsorption–desorption experiment is a popular method to examine the porous materials. The isotherms arising from HZSM-5, HZSM-5-AT, Mg (1 wt%)-H and Mg (1 wt%)-AT are displayed in Fig. 1. The isotherms of the four samples are similar with a hysteresis loop at relatively high pressure (P/P_0), indicating that the four samples present a relatively high external surface area with a little mesoporousity.[34] The isotherm specific to Mg (1 wt%)-AT became narrow and moved to high pressure a little bit compared with that of the HZSM-5, illustrating that the surface area of microporous decreased owing to the dual modification of Mg and alkali.[4]

The texture properties of the catalysts HZSM-5, Mg (1 wt%)-H, HZSM-5-AT and Mg (1 wt%)-AT are shown in Table 1. The average pore size of sample HZSM-5-AT was found to be the largest. The modification of the catalyst HZSM-5 with alkali-treatment would increase the ratio of surface area of mesopores to BET surface area. The modification of the catalyst HZSM-5 with MgO led to decreasing in the BET surface area of HZSM-5. Some research group insisted that zeolite micropores would be filled by magnesium oxide.[28] The alkali-treatment apparently has a pronounced effect on the pore properties of HZSM-5, removed framework Al during the process, and partially destroyed micropores. Furthermore, Mg-loading after alkali-treatment could proceed with micropores destroying and

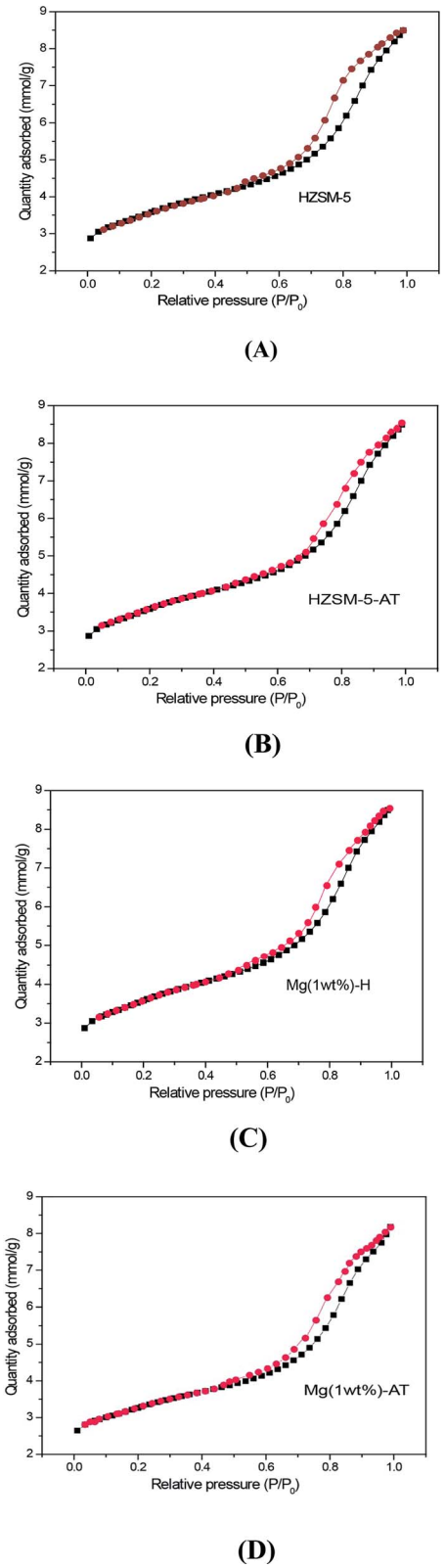

Fig. 1 N_2 adsorption–desorption isotherms of the catalysts. (A) HZSM-5; (B) HZSM-5-AT; (C) Mg (1 wt%)-H; (D) Mg (1 wt%)-AT.

blocking. After HZSM-5 was modified by both magnesium doping and alkali treatment the ratio of surface area of mesopores to the BET surface area was found to be the highest, indicating the dual modification method could alter the ratio of the surface area of mesopores to total surface area. Alkali-treatment obviously enlarged the pore-size while the promoter Mg would continue expanding the pore-size.[28] The enhancement in selectivity and productivity of ethylbenzene over Mg (1 wt%)-AT could be explained in terms of the destruction of micropores while the mesopores was improved by alkali treatment and magnesium doping.

XRD patterns of the HZSM-5, Mg (1 wt%)-H, HZSM-5-AT and Mg (1 wt%)-AT catalysts are shown in Fig. 2; the two diffraction peaks at $2\theta = 7^\circ$ and 10° and three diffraction peaks at $2\theta = 22.5^\circ$, 23.5° and 25° were corresponding to (010), (020), (501), (151) and (303) crystal faces of HZSM-5 molecular sieves (MFI structure).

It can be seen that the modification with alkali and/or Mg did not alter the HZSM-5 crystal structure. In addition, no patterns specific to MgO crystalline were detected from the XRD spectra. This result indicated that MgO might be highly dispersed on the surface of HZSM-5.

The images in Fig. 3a–c are specific to HZSM-5 zeolite, the HZSM-5 zeolite treated by 0.2 M NaOH solution for 3 h at 338 K, and the one modified with both alkali and Mg (1 wt%), respectively. Comparing the images in Fig. 3a and b, some cracks and faults on the surface of HZSM-5-AT particles can be found. The zeolite grain was partially fragmentized owing to the alkali-treatment under these conditions. Compared Fig. 3b and c, the particle sizes of the sample Mg (1 wt%)-AT were found to be small and more homogeneous, indicating that Mg improved the surface structure of the catalyst.

Fig. 4 shows the ^{27}Al MAS NMR spectra of all the samples. Compared the ^{27}Al MAS NMR spectra between Fig. 4(A) and (B), it could conclude that both Mg doping and alkali treatment play important role in the modification of zeolite. As shown in Fig. 4(A), with chemical shifts two peaks at around 54 and -4 ppm were typically observed for HZSM-5 zeolite, which were assigned to the framework Al (FAL) and extra-framework Al oxide (EFAL) species, respectively. In Fig. 4(B), for the samples modified with Mg alone, the peak at -4 ppm disappeared. Similar observations were also reported by Mao *et al.* and Zheng *et al.*[9,28] The NMR characterization results confirmed that the disappearance of the peak at -4 ppm after Mg modification did not result from a partial dealumination, this is because of removal of Al from T atom positions of the zeolite, suggesting a strong interaction of MgO with EFAL. Woolery *et al.*[35] considered that EFAL was relative to Brønsted acid and Lewis acid. This conclusion would be demonstrated by pyridine adsorbed FT-IR experiment results. As presented in Scheme 1,[28,29] after partial dealumination and desilicification caused by Mg doping and alkali treatment, Mg substituted for hydroxyl group in the structure of HZSM-5. The alkali-treatment would contribute to the formation of more extra framework Al. Moreover, the increase in the number of Lewis acid sites caused by a strong interaction of Mg $(OH)^+$ with EFAL was found to be very evident.

Mg (1 wt%)-AT in Fig. 4(A) still existed relative weak peak at -4 ppm compared with Mg (1 wt%)-H in Fig. 4(B). It illustrated that the EFAL species were strengthen by alkali-treatment and had a positive relation to the ratio of Lewis acid to Brønsted acid.

Table 1 Influence of Mg promoter on texture properties of ZSM-5

Samples	S_{BET}[a] ($m^2\ g^{-1}$)	V_{total}[c] ($cm^3\ g^{-1}$)	V_{micro}[c] ($cm^3\ g^{-1}$)	S_{micro}[c] ($m^2\ g^{-1}$)	V_{micro}[c]/V_{total}[b] (%)	S_{meso}[b]/S_{BET}[a] (%)	D_{aver}[c] (nm)
HZSM-5	251	0.325	0.108	140	33.3	52	6.20
Mg (1 wt%)-H	271	0.284	0.092	120	32.3	52	6.33
HZSM-5-AT	285	0.335	0.094	121	28.0	64	6.55
Mg (1 wt%)-AT	306	0.328	0.089	112	27.1	94	6.96

[a] BET Method. [b] BJH method. [c] *t*-plot method; D_{aver}: average pore size.

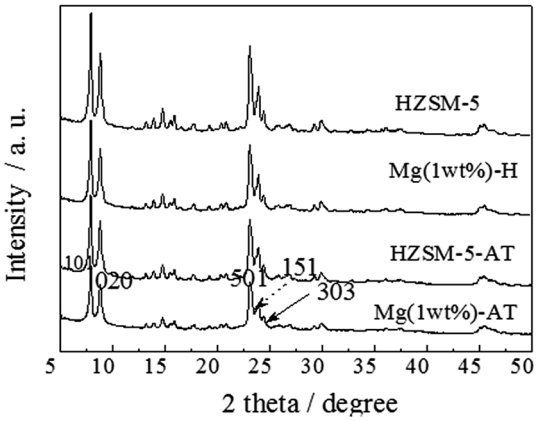

Fig. 2 XRD patterns of H-ZSM-5 zeolites modified by alkali treatment and/or Mg doping.

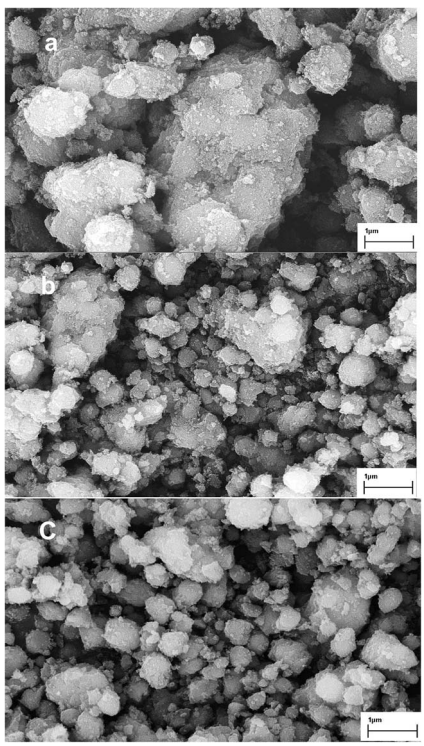

Fig. 3 SEM images of different catalysts.

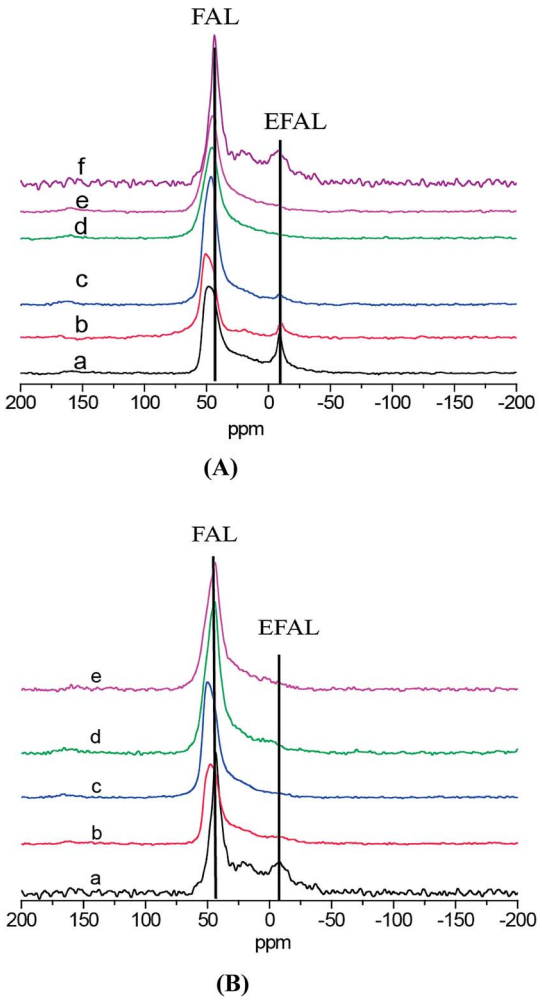

Fig. 4 ^{27}Al MAS NMR spectra of all the samples.

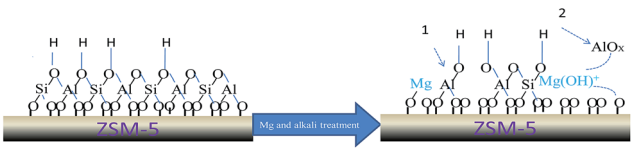

Scheme 1 The formation of Lewis acid sites by alkali-treatment and Mg-promoting: (1) framework Al Lewis site, (2) extra framework Al Lewis site.

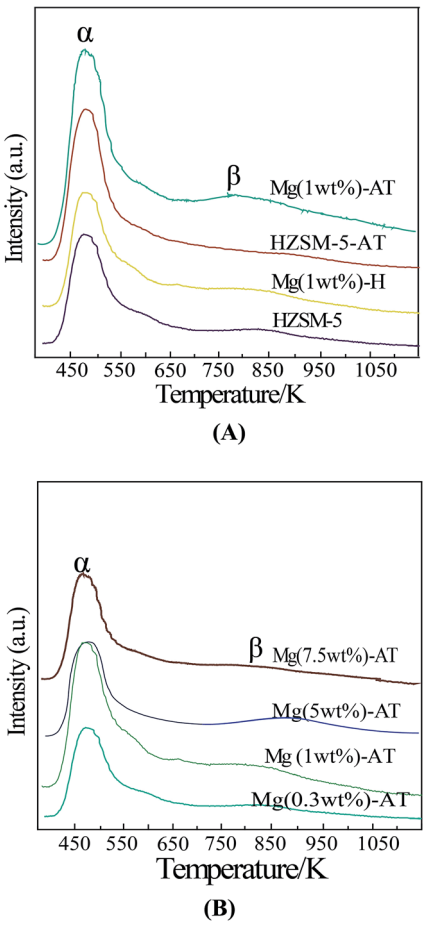

Fig. 5 NH_3-TPD spectra of the samples.

3.2 Acid characterization

Fig. 5 shows the NH_3-TPD curves of all the catalyst samples. The Mg (1 wt%)-H, Mg (1 wt%)-AT, HZSM-5, HZSM-5-AT, Mg (0.3 wt%)-AT, Mg (5 wt%)-AT, Mg (7.5 wt%)-AT catalyst samples exhibit two desorption peaks at 473 K and 793 K, which were labeled α and β, respectively. Peak α represents weak acid sites on the ZSM-5 surface, peak β represents strong acid site in the structure.[19]

The quantitative values of acidity of the samples are shown in Table 2. The quantitative value of acidity of HZSM-5 (the mole ratio of SiO_2 to Al_2O_3 equals to 80) was reported elsewhere to be 0.348 mmol NH_3 per g cat.[36,37] Compared with the value of the acidity of HZSM-5, the quantitative value of acidity of other samples could be calculated. In Table 2, the weak acidity of HZSM-5-AT, Mg (1 wt%)-H, Mg (0.3 wt%)-AT, Mg (1 wt%)-AT, Mg (5 wt%)-AT and Mg (7.5 wt%)-AT increased, while the sample Mg (1 wt%)-AT had the highest peak area of weak acidity. As reported by Beyer, the strength of Lewis acidic sites is associated with the EFAL species.[38] Our results of FI-IR and MAS NMR confirmed this view. The sequence of the ratios of Lewis acid to Brønsted acid was found to be Mg (1 wt%)-AT > Mg (0.3 wt%)-AT > Mg (7.5 wt%)-AT > Mg (5 wt%)-AT > Mg (1 wt%)-H > HZSM-AT > HZSM-5, which is relative to the EB productivity.

The pyridine-adsorbed IR spectra arising from HZSM-5, HZSM-5-AT, Mg (1 wt%)-H Mg (0.3 wt%)-H, Mg (5 wt%)-H, Mg (7.5 wt%)-H Mg (1 wt%)-AT, Mg (0.3 wt%)-AT, Mg (5 wt%)-AT and Mg (7.5 wt%)-AT are shown in Fig. 6. The FT-IR spectra of pyridine adsorbed on HZSM-5 exhibit the characteristic bands at 1550 cm^{-1} and 1450 cm^{-1}, which are attributed to pyridinium ions chemisorbed on Brønsted acid sites and coordinately bound pyridine with Lewis acid sites, respectively.[36–40]

Mao[19] found that when Mg loading is 2.5 wt%, the ratio of Lewis acid to Brønsted acid is the highest. However, when Mg loading is more than 5 wt%, both Lewis and Brønsted acid decreased. It was reported that $Mg(OH)^+$ which was one of influence factors of Lewis acid site (see Scheme 1) would condense to form MgO when the loading of MgO reaches 10 wt%; thus the amounts of both Brønsted acid and Lewis acid decrease.[19] In this study, the sample Mg (1 wt%)-AT exhibits the highest *L*/*B* ratio, and presented the highest activity and selectivity to EB. Furthermore, the variation sequence of the ratio of *L*/*B* acid agreed with EB productivity. It could be concluded that high activity and selectivity to EB is due to the proper *L*/*B* acid proportion.

3.3 Alkylation of benzene with ethanol over different catalysts

As presented in Scheme 2, ethanol is protonated by Brønsted acid site and Lewis acid site to carbenium ion, which is attacked subsequently by a free or weakly adsorbed benzene molecule, leading to producing ethylbenzene.

The activity data of the Mg-AT and Mg-H samples with different loadings of Mg are shown in Table 3. From Table 3 the highest activity was observed over Mg-HZSM-5-AT when the loading of Mg on HZSM-5-AT was 1 wt%. Further increasing in Mg content over 5 wt% resulted in the decrease in the selectivity

Table 2 NH_3-TPD and Py-IR results of the calcined samples

Sample	Weak acid (mmol NH_3 per g cat.)	Strong acid (mmol NH_3 per g cat.)	Total acid (mmol NH_3 per g cat.)	*L* acid[a]	*B* acid[a]	*L*/*B*[a]
HZSM-5	0.199	0.149	0.348	54.3	18.9	2.87
HZSM-5-AT	0.229	0.128	0.357	89.9	27.8	3.23
Mg (1 wt%)-H	0.257	0.104	0.361	70.2	27.8	2.52
Mg (1 wt%)-AT	0.400	0.248	0.648	110	29.0	3.79

[a] The relative value of Brønsted acid and Lewis acid sites, estimated from the corresponding calibrated peak areas.

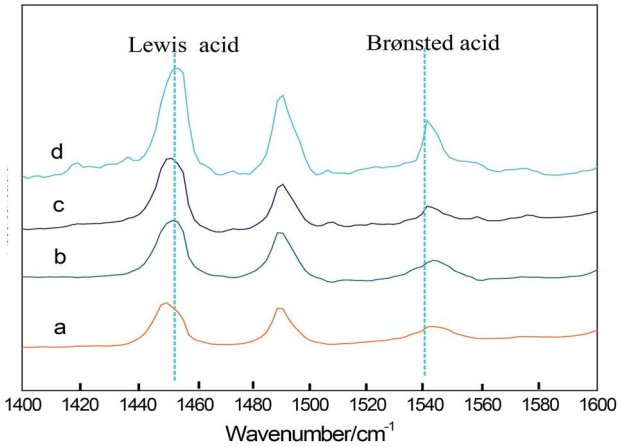

(A)

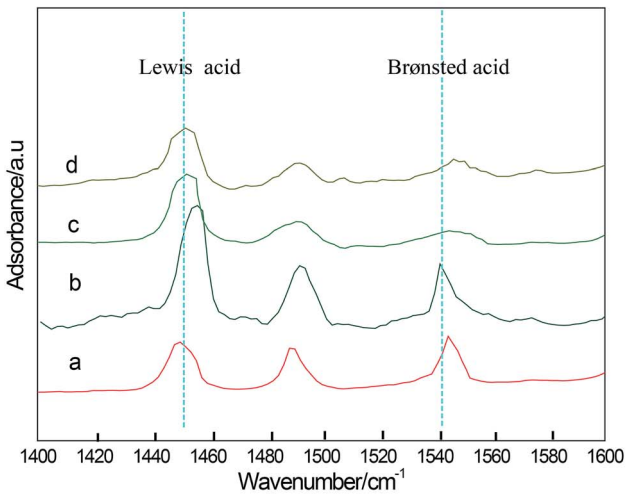

(B)

Fig. 6 Pyridine-adsorbed FT-IR spectra of the samples.

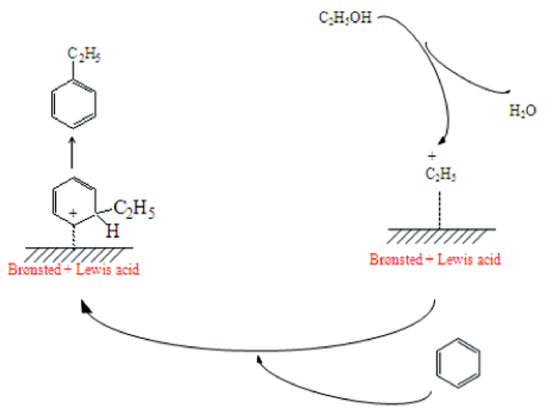

Scheme 2 Proposed overall reaction scheme during benzene alkylation.

Table 3 Catalytic activity and product selectivity as a function of Mg loading[a]

	Conversion of benzene%	Selectivity to ethylbenzene%	Productivity of ethylbenzene%
HZSM-5	24	91	22
HZSM-5-AT	26	89	23
Mg (0.3 wt%)-AT	28	91	25
Mg (1 wt%)-AT	30	92	28
Mg (5 wt%)-AT	26	88	23
Mg (7.5 wt%)-AT	26	85	24
Mg (0.3 wt%)-H	24	86	21
Mg (1 wt%)-H	26	89	23
Mg (5 wt%)-H	26	86	22
Mg (7.5 wt%)-H	26	83	22

[a] Reaction condition: temperature at 658 K, WHSV 4 h^{-1}, time-on-stream 10 h.

toward ethylbenzene and the conversion of benzene. It might result in the decrease of both Lewis and Brønsted acid.[19] Compared the activity of Mg (0.3 wt%)-H, Mg (1 wt%)-H, Mg (5 wt%)-H and Mg (7.5 wt%)-H with those of Mg (0.3 wt%)-AT, Mg (1 wt%)-AT, Mg (5 wt%)-AT and Mg (7.5 wt%)-AT, it could be found that Mg promoter improved the HZSM-5 catalyst only when it had been alkali-treated previously. Both the amount of Lewis and Brønsted acid sites and the amount ratio of *L*/*B* are important for the reaction.

The long-term stability and activity of the catalyst is vital for industrial application. Catalytic activity as a function of time on stream for Mg (1 wt%)-AT is displayed in Fig. 7. The Mg (1 wt%)-AT catalyst showed excellent catalytic performance at 658 K with 100 h time on stream stable. It can be observed from Fig. 7 that the conversion of benzene was 26.6% at the beginning during the reaction process, and then increased slowly. After 30 h on stream, the conversion of benzene increased to 29.1%; after 65 h reaction, the conversion of benzene was stable at 28.5% or so; the selectivity toward ethylbenzene remained relatively stable at almost 90.4%. All the activity data for alkylation reaction were measured with error bar ±3%.

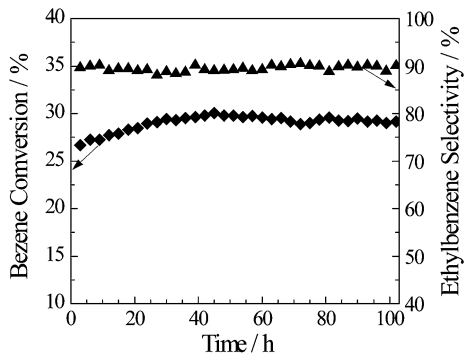

Fig. 7 Catalytic performance of Mg (1 wt%)-AT as a function of time on stream.

4. Conclusions

Dual modification of H-ZSM-5 by alkali treating and Mg doping gave rise to partial dealumination and desilicification of the catalyst, promoting the formation of extra mesopores. The substitution of Mg for hydroxyl group led to forming $Mg(OH)^+$; while alkali treatment would contributed to the formation of more extra framework Al (EFAL). The strong interaction between Mg $(OH)^+$ and EFAL results in the increase of the amount of Lewis acid sites, which was believed to be active site for benzene alkylation with ethanol. It was found higher *L*/*B* ratio facilitates the improvement of the activity of the catalyst and selectivity toward EB. The sample Mg (1 wt%)-AT exhibits the highest *L*/*B* ratio (3.79), and presented the highest productivity (30%) and selectivity to EB (92%).

References

1 Y. J. Zhang, D. B. Li and S. J. Zhang, *RSC Adv.*, 2009, **32**, 16391–16396.
2 V. R. Vijayaraghavan, K. Joseph and R. Antony, *J. Mol. Catal. A: Chem.*, 2004, **41**, 207–214.
3 A. Corma, *Chem. Rev.*, 1997, **97**, 2373–2386.
4 W. Z. Zhang, F. Xu and D. J. Wang, *RSC Adv.*, 2014, **32**, 16528–16536.
5 W. J. Zhang, F. F. Bi, Y. Yu and B. He, *J. Mol. Catal. A: Chem.*, 2013, **37**, 26–29.
6 S. C. Qi, L. Zhang, X. Y. Wei, J. Hayashi, Z. M. Zong and L. L. Guo, *RSC Adv.*, 2014, **33**, 17105–17109.
7 M. Takeuchi, M. Hidaka and M. Anpo, *J. Hazard. Mater.*, 2012, **237**, 133–145.
8 G. T. Kokotailo, S. L. Lawton and D. H. Olson, *Nature*, 1978, **272**, 10–15.
9 S. Zheng, J. Anderas and A. L. Johannes, *J. Catal.*, 2003, **219**, 11–18.
10 S. M. Cricsery, *Zeolites*, 1984, **4**, 12–20.
11 M. A. Camblor, A. Corma and S. Valenica, *Microporous Mesoporous Mater.*, 1998, **25**, 3–9.
12 J. R. Anderson, T. Mole and V. Christov, *J. Catal.*, 1980, **61**, 477–484.
13 A. W. Fort and B. H. Davis, *J. Catal.*, 1985, **96**, 357–367.
14 Y. Sugi, Y. Kubota and K. Kumura, *Appl. Catal., A*, 2006, **299**, 157–166.
15 C. T. Kresge, M. E. Lenowicz and W. J. Roth, *Nature*, 1992, **359**, 12–19.
16 S. K. Seong, W. Zhang and J. Thomas, *Science*, 1998, **282**, 1302–1305.
17 A. Karsson, M. Stcker and R. Schmidt, *Microporous Mesoporous Mater.*, 1999, **27**, 181–192.
18 L. Huang, W. Guo and P. Deng, *J. Phys. Chem. B*, 2000, **104**, 2817–2823.
19 R. L. V. Mao, S. Xiao, A. Ramsaran and J. Yao, *J. Mater. Chem.*, 1994, **4**, 605–613.
20 C. S. Cundy, M. S. Henty and R. J. Plaisted, *Zeolites*, 1995, **15**, 342–354.
21 A. Cizmek, B. Subotic, R. Aiello, F. Crea, A. Nastro and C. Tuoto, *Microporous Mater.*, 1995, **4**, 159–168.
22 M. Ogura, S. Shinomiya, J. Tateno, Y. Nara, E. Kikuchi and M. Matsukata, *Chem. Lett.*, 2000, **7**, 882–896.
23 J. M. Maselli and A. W. Peters, *Catal. Rev.: Sci. Eng.*, 1984, **256**, 25–33.
24 P. Lersch and F. Bandermann, *Appl. Catal.*, 1991, **75**, 133–145.
25 Y. Li, W. Xie and S. Yong, *Appl. Catal., A*, 1997, **50**, 231–247.
26 P. Kovacheva, A. Predoeva, K. Arishtirova and S. Vassilev, *Appl. Catal., A*, 2002, **223**, 121–134.
27 M. T. Sami, B. M. Almutairi, C. M. M. Pieter, A. P. Evgeny and J. M. H. Emiel, *ACS Catal.*, 2012, **2**, 71–79.
28 D. S. Mao, W. M. Yang, J. C. Xia, B. Zhang, Q. Y. Song and Q. L. Chen, *J. Catal.*, 2005, **230**, 140–149.
29 L. Zhao, J. Gao and C. Xu, *Fuel Process. Technol.*, 2011, **92**, 414–423.
30 J. J. Li, Y. H. Gan, W. M. Wang, W. P. Fang and Y. Q. Yang, *J. Xiamen Univ., Nat. Sci.*, 2012, **51**, 882–897.
31 J. Wang, B. Y. Zhao and Y. C. Xie, *Acta Phys.-Chim. Sin.*, 2001, **179**, 66.
32 B. M. Lin, Q. H. Zhang and Y. Wang, *Ind. Eng. Chem. Res.*, 2009, **48**, 10788–10794.
33 T. Kawai, K. M. Jiang and T. Ishikawa, *J. Catal.*, 1996, **159**, 288–298.
34 A. Corma, U. Diaz, V. Fornes, J. M. Guil, J. M. Triguero and E. J. Ceyghtony, *J. Catal.*, 2000, **191**, 218–224.
35 G. L. Woolery, G. H. Kuehl, H. C. Timken, A. W. Chester and J. C. Vartuli, *Zeolites*, 1997, **19**, 288–296.
36 R. Ueda, T. Kusakari, K. Tomishige and K. Fujimoto, *J. Catal.*, 2000, **194**, 14–20.
37 A. G. Gayubo, A. T. Aguayo, A. Atutxa, R. Prieto and J. Bilbao, *Ind. Eng. Chem. Res.*, 2004, **43**, 5042–5053.
38 P. A. Jacobs and H. K. Beyer, *J. Phys. Chem.*, 1979, **83**, 1174–1177.
39 N. Y. Topsoe, K. Pedersen and E. G. Derouane, *J. Catal.*, 1981, **70**, 41–49.
40 C. A. Emeis, *J. Catal.*, 1993, **141**, 347–358.